

# Hoyle state and rotational features in Carbon-12 within a no-core shell model framework

Alison C. Dreyfuss

Keene State College, Keene, New Hampshire 03435, USA

Kristina D. Launey, Tomáš Dytrych, and Jerry P. Draayer

Department of Physics and Astronomy, Louisiana State University, Baton Rouge, LA 70803, USA

Chairul Bahri

Department of Physics, University of Notre Dame, Notre Dame, Indiana 46556-5670, USA

By using only a fraction of the model space extended beyond current no-core shell-model limits and a schematic effective many-nucleon interaction, we gain additional insight within a symmetry-guided shell-model framework, into the many-body dynamics that gives rise to the ground state rotational band together with phenomena tied to alpha-clustering substructures in the low-lying states in  $^{12}\text{C}$ , and in particular, the challenging Hoyle state and its first  $2^+$  excitation. For these states, we offer a novel perspective emerging out of no-core shell-model considerations, including a discussion of associated nuclear shapes and matter radii. This, in turn, provides guidance for *ab initio* shell models by informing key features of nuclear structure and the interaction.

Our present-day knowledge of various phenomena of astrophysical significance, such as nucleosynthesis, the evolution of primordial stars in the Universe, and X-ray bursts depends on reaction rates for the stellar triple- $\alpha$  process, which can considerably affect, e.g., results of core-collapse supernovae simulations and stellar evolution models, predictions regarding X-ray bursts, as well as estimates of carbon production in asymptotic giant branch (AGB) stars [1]. These rates, in turn, are greatly influenced by accurate measurements and theoretical predictions of several important low-lying states in  $^{12}\text{C}$ , including the second  $0_2^+$  (Hoyle) state and its  $2^+$  excitation that continues to foster debate in experimental studies [2–6]. Further challenges relate to the long-recognized alpha-cluster substructure of these states that has been limited to explorations by cluster-tailored [7, 8] or self-consistent [9] microscopic methods. Indeed, these highly deformed patterns have hitherto precluded an accurate – from first principles – no core shell-model (NCSM) description of the Hoyle state and its rotational band [10], and, only recently, first *ab initio* state-of-the-art calculations have been attempted using effective field theory (EFT) and a coarse lattice [11].

In this letter, we report on a first study of these phenomena in  $^{12}\text{C}$  within a no-core shell-model framework with essentially no limitation on the number of harmonic oscillator (HO) shells included in the model space. While such model spaces remain inaccessible by *ab initio* shell models, we are able to address a long-standing challenge [12], namely, understanding highly-deformed spatial configurations from a shell-model perspective. Furthermore, this study allows one to gain further insight into the many-body dynamics, including the physically relevant shape deformations and particle-hole configurations, that gives rise to the ground state (*g.st.*) rotational band (the

lowest  $0^+$ ,  $2^+$  and  $4^+$  states) together with low-lying states suggested to have a cluster structure ( $0_2^+$  Hoyle state and its  $2^+$  excitation), as well as a third low-lying  $0_3^+$  state in  $^{12}\text{C}$ . This analysis greatly benefits from the use of a schematic, but fully microscopic, effective many-nucleon interaction and is based on the close agreement of model outcomes with experiment – including excitation energies and other observables such as mass rms radii, electric quadrupole moments and  $E2$  transition rates – as well as to wavefunctions obtained by *ab initio* no-core shell model (NCSM) calculations [13] with the JISP16 realistic nucleon-nucleon ( $NN$ ) interaction [14].

Above all, the qualitative results of the present study provide guidance for *ab initio* shell model approaches by informing key features of nuclear structure and the interaction. In particular, for a description of alpha-cluster phenomena, the outcome points to the need for simple effective interactions beyond two-body realistic ones, and manifests a clear indication that achieving *ab initio* descriptions is within the reach of the NCSM. The latter, in turn, will bring forward an accurate reproduction and reliable prediction of energy spectra and associated transition rates that majorly impact astrophysical studies.

**Symmetry-adapted shell-model framework.** – We employ the no-core symplectic model (NCSpm) for symmetry-preserving interactions with  $\text{Sp}(3, \mathbb{R})$  the underpinning symmetry [15]. This symmetry is indeed found inherent to nuclear dynamics – a result we have demonstrated in an analysis of large-scale *ab initio* NCSM applications for  $^{12}\text{C}$  and  $^{16}\text{O}$  [16]. The model offers a microscopic description of  $A$  nucleons in terms of mixed shape deformations, directly related to particle relative (with respect to the center of mass, CM) position and momentum coordinates,  $\mathbf{r}_i$  and  $\mathbf{p}_i$ , with  $i = 1, \dots, A$ . It has been successfully applied to  $^{166}\text{Er}$  using Davidson

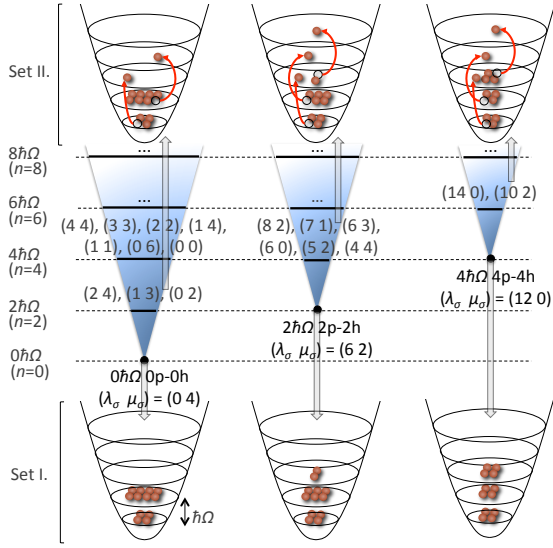


FIG. 1:  $\text{Sp}(3, \mathbb{R})$  irreps (slices) that comprise the model space used for the  $^{12}\text{C}$  NCSpm calculations. Basis states  $(\lambda\mu)$  of a slice are built by  $2\hbar\Omega$  1p-1h monopole or quadrupole excitations (set II) over a bandhead. The symplectic bandhead (set I) is a  $\text{SU}(3)$ -coupled many-body state with a given nucleon distribution over the HO shells. The corresponding HO energy of this nucleon configuration together with the bandhead shape,  $(\lambda_\sigma \mu_\sigma)$ , serve to label the symplectic irrep.

potential [17] and is a microscopic realization of the Bohr-Mottelson collective model [18], as well as a multiple HO shell generalization of Elliott's  $\text{SU}(3)$  model [19].

The NCSpm utilizes a symplectic basis (for details, see [20]), which is related – via a unitary transformation – to the three-dimensional HO ( $m$ -scheme) many-body basis used in the NCSM [21]. The conventional NCSM basis spaces are constructed using HO single-particle states and are characterized by the  $\hbar\Omega$  oscillator strength as well as by the cutoff in total oscillator quanta,  $N_{\text{max}}$ , above the lowest energy configuration for a given nucleus. Indeed, the NCSpm employed within a full model space up through  $N_{\text{max}}$ , will coincide with the NCSM for the same  $N_{\text{max}}$  cutoff. It is therefore clear that the present study, while down-selecting to the most relevant configurations, provides the first shell-model calculations carried beyond current NCSM limits, namely, up through  $N_{\text{max}} = 20$ , the model space we found sufficient for the convergence of results. These important configurations are chosen among all possible symplectic  $\text{Sp}(3, \mathbb{R})$  irreducible representations (irreps) within the model space.

The  $\text{Sp}(3, \mathbb{R})$  irreps divide the space into ‘vertical slices’ that are comprised of basis states of a definite shape specified by the deformation  $(\lambda\mu)$  quantum numbers of  $\text{SU}(3)$ , which is embedded in  $\text{Sp}(3, \mathbb{R})$  (Fig. 1). The simplest cases, namely,  $(00)$ ,  $(\lambda 0)$ , and  $(0\mu)$ , describe a spherical, prolate, and oblate shape, respectively, while a general nuclear state is typically a superposition of sev-

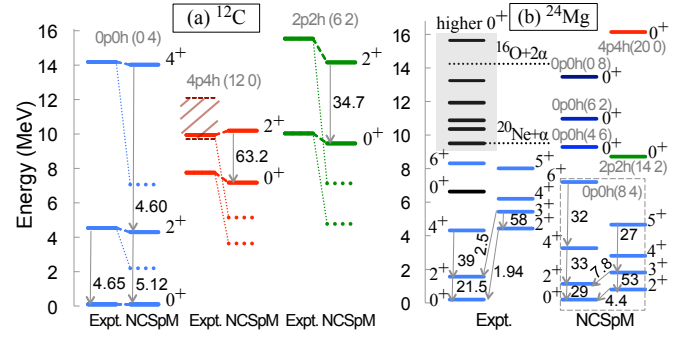


FIG. 2: NCSpm energy spectrum of (a)  $^{12}\text{C}$ , not scaled (dotted) and rescaled (solid), and (b)  $^{24}\text{Mg}$  (not scaled). Experimental energies for all states are from [29], except the latest results for the  $^{12}\text{C}$   $0_3^+$  and  $2_2^+$  [4] (shaded area shows the  $2_2^+$  energy range from [2–6]).  $B(E2)$  transition rates are in W.u.

eral hundred various triaxial shapes. The basis states are built over a bandhead (Fig. 1, Set I) by consecutive  $2\hbar\Omega$  1p-1h (1-particle-1-hole) excitations (Fig. 1, Set II), together with a smaller  $2\hbar\Omega$  2p-2h correction for eliminating the spurious CM motion (not shown in the figure). In NCSpm, to eliminate the spurious CM motion, we use symplectic generators constructed in relative coordinates with respect to the CM. These generators are used to build the basis, the interaction, the many-particle kinetic energy operator, as well as to evaluate observables.

We note that the NCSpm, as presented here, is limited to interactions that preserve the  $\text{Sp}(3, \mathbb{R})$  symmetry. While this greatly facilitates the use of a group-theoretical apparatus and analytical expressions for the Hamiltonian matrix elements, which, in turn, makes large  $N_{\text{max}}$  spaces possible to manage, *ab initio* calculations lie beyond the scope of the current model. The addition of symmetry-mixing terms in the interaction is feasible and a logical extension of the theory that is under development. Nonetheless,  $\text{Sp}(3, \mathbb{R})$ -symmetric Hamiltonians appear to be particularly suitable to capture the essential characteristics of the low-energy nuclear kinematics and dynamics. The reason is that such Hamiltonians can include the many-particle kinetic energy,  $\sum_i \mathbf{p}_i^2 / (2m)$ , the HO potential,  $\sum_i m\Omega^2 \mathbf{r}_i^2 / 2$ , as well as terms dependent on the orbital momentum,  $\mathbf{L} = \sum_i \mathbf{r}_i \times \mathbf{p}_i$ , and terms dependent on the mass quadrupole moment,  $Q_{2\mu} = \sum_i q_{2\mu}(i) = \sum_i \sqrt{16\pi/5} r_i^2 Y_{2\mu}(\hat{\mathbf{r}}_i)$ , such as the important interaction of each particle with the total quadrupole moment of the system,  $\frac{1}{2} \mathbf{Q} \cdot \mathbf{Q} = \frac{1}{2} \sum_i q(i) \cdot (\sum_j q(j))$  [18].

For the purposes of this study, we utilize a novel microscopic many-body interaction suitable for large- $N_{\text{max}}$  no-core shell models, which is tied to the long-range expansion of the nucleon-nucleon central force  $V(|\mathbf{r}_i - \mathbf{r}_j|)$  (for a derivation, see [22]) and kept as simple as possible by considering the most relevant degrees of freedom for

a description of highly deformed spatial configurations, namely, coupling of single-particle  $q_{2\mu}(i)$  quadrupole HO excitations,

$$H_\gamma = \sum_{i=1}^A \left( \frac{\mathbf{p}_i^2}{2m} + \frac{m\Omega^2 \mathbf{r}_i^2}{2} \right) - \frac{\chi (e^{\gamma Q \cdot Q} - 1)}{\gamma}, \quad (1)$$

given in terms of particle coordinates relative to the CM<sup>1</sup>. We take the coupling constant  $\chi = \hbar\Omega/(4\sqrt{N_f N_i})$  with  $N_{f(i)}$  the total HO quanta of the final (initial) many-body basis state. The decrease of  $\chi$  with  $N$ , to a leading order, has been shown by Rowe [25] based on self-consistent arguments and used in an  $\text{Sp}(3, \mathbb{R})$ -based study of cluster states of  $^{16}\text{O}$  [26]. It is worth noting that such a choice for  $\chi$  renders the eigenstates of  $H_\gamma$   $\hbar\Omega$ -independent. Above all, the  $H_\gamma$  introduces simple but important many-body interactions that enter in a prescribed hierarchical way given in powers of a small negative parameter  $\gamma$ , the only adjustable parameter in the model.

The NCSpM, with  $H_\gamma$ , reduces to the established Elliott model [19] in the limit of a single valence shell and zero  $\gamma$ . In this limit, the model was shown to effectively describe rotational features of light nuclei [19]. A successful extension to multiple shells has been achieved and applied to the  $^{24}\text{Mg}$  *g.st.* rotational band [27], where an interaction given as a polynomial in  $Q$  up through  $(Q \cdot Q)^2$  was employed. Such an interaction directly ties to our effective Hamiltonian (1). In addition, Eq. (1) could be understood in terms of a renormalization (e.g., see [28]) of the  $\chi$  coupling constant of the  $\frac{1}{2} \sum_{ij} q(i) \cdot q(j)$   $NN$  interaction, *i.e.*,  $\frac{\chi}{2} (e^{\gamma Q \cdot Q} - 1)/\gamma = \frac{1}{2} [\chi (\sum_{k=0}^{\infty} \frac{\gamma^k (Q \cdot Q)^k}{(k+1)!})] Q \cdot Q$ , where higher-order terms become quickly negligible for a reasonably small  $\gamma$  and, e.g., for  $^{12}\text{C}$  only terms up through  $k = 1$  (*g.st.*) or  $k = 3$  (Hoyle state) are found sufficient.

**Energy spectrum for  $^{12}\text{C}$  and comparison to *ab initio* results.** — As the interaction and the model space are carefully selected to reflect the most relevant physics, the outcome reveals a quite remarkable agreement with experiment. The low-lying energy spectrum and eigenstates for  $^{12}\text{C}$  were calculated using the NCSpM with  $H_\gamma$  of Eq. (1) for  $\hbar\Omega = 18$  MeV given by the empirical estimate  $\approx 41/A^{1/3} = 17.9$  MeV. The results are shown for  $N_{\text{max}} = 20$ , which we found sufficient to yield convergence. This  $N_{\text{max}}$  model space is further reduced by selecting the most relevant symplectic irreps (Fig. 1), namely, the spin-zero ( $S = 0$ )  $0\hbar\Omega$  0p-0h (04),  $2\hbar\Omega$  2p-2h (62), and  $4\hbar\Omega$  4p-4h (120) symplectic bandheads together with all multiples thereof up through  $N_{\text{max}} = 20$

of total dimensionality of  $4.5 \times 10^3$ . In comparison to the experimental energy spectrum (Fig. 2a), the outcome reveals that, for  $\gamma = -1.71 \times 10^{-4}$ , the lowest  $0^+$ ,  $2^+$ , and  $4^+$  states of the  $0\hbar\Omega$  0p-0h (04) symplectic irrep closely reproduce the *g.st.* rotational band; the  $4\hbar\Omega$  4p-4h (120) irrep successfully describes the Hoyle state and its rotational structure, while the calculated lowest  $0^+$  of the  $2\hbar\Omega$  2p-2h (62) is found to lie close to the 10-MeV  $0^+$  resonance (third  $0^+$ ) observed in  $^{12}\text{C}$ . We note that our model yields a rather compressed spectrum (Figure 2a, dotted-line states) with a small  $0_{g.st.}^+ - 2_1^+$  spacing as the one calculated by early cluster models, which remedy this by allowing for alpha-cluster dissociation due to a spin-orbit force as discussed in Ref. [30]. However, an overall factor of two brings all the NCSpM states under consideration remarkably close to the experimental values (Figure 2a, solid-line states). This scaling has no effect on the underlying physics, as also shown next, because an overall factor for  $H_\gamma$  does not change its properties and eigenstates, or other associated observables.

A close similarity is observed when the probability distributions for the *g.st.* rotational band are compared to *ab initio* results when only configurations of zero proton and neutron spins ( $S_{p,n} = 0$ ) are selected (for  $0_{g.st.}^+$ , see Fig. 3a). In particular, NCSpM eigenstates, which are  $\hbar\Omega$ -independent, are compared to symmetry-adapted no-core shell model (SA-NCSM) calculations [13] with bare JISP16 realistic interaction for  $\hbar\Omega = 20$  MeV (around the minimum of the calculated binding energy for  $^{12}\text{C}$ ) and an  $N_{\text{max}} = 8$  model space. This space appears to be sufficient to yield convergent results for the *g.st.* rotational band for both models. The close agreement shows that among all possible  $S_{p,n} = 0$  configurations present in the SA-NCSM, only the states of the (04) slice used here appear dominant. It also points to the fact that the schematic interaction used in NCSpM has effectively captured most of the underlying physics of the realistic interaction important to the low-energy nuclear dynamics. Indeed, for the same  $N_{\text{max}}$  and  $\hbar\Omega$ , NCSpM observables, such as *g.st.* matter rms radius,  $B(E2; 2_1^+ \rightarrow 0_{g.st.}^+)$ , and  $Q_{2_1^+}$ , reproduce the *ab initio* counterparts as much as 91%, 83%, and 80%, respectively.

For the Hoyle state and its rotational band, larger spaces are needed, e.g., nonnegligible configurations extend to  $N_{\text{max}} = 18$  (Fig. 3b), which is within a reach of next-generation NCSM models. While the predominant component of the lowest  $0^+$  state is at  $0\hbar\Omega$  ( $n = 0$ ) and manifests an evident oblate shape, the Hoyle state peaks around  $8\hbar\Omega$  ( $n = 8$ ) with a clear evidence for a prolate shape deformation with (160) being the largest contribution. Moreover, this state emerges from a 4p-4h shell-model configuration, that is, the (120) bandhead (Fig. 1, set I) is realized by an alpha-particle configuration – spatially spherical (00), spin zero, and isospin zero – in each of the three lowest HO shells (implying spatial displacement). This together with the strong prolate de-

<sup>1</sup> Although a technical detail, it is important to note that  $Q \cdot Q$  in this expression denotes the  $Q \cdot Q - \langle Q \cdot Q \rangle_n$  interaction, where the  $\langle Q \cdot Q \rangle_n$  term is subtracted from  $Q \cdot Q$  to eliminate a spurious shift in the zero-point energy by the average contribution,  $\langle Q \cdot Q \rangle_n$ , of  $Q \cdot Q$  within the subspace of  $n$  HO excitations [23, 24].

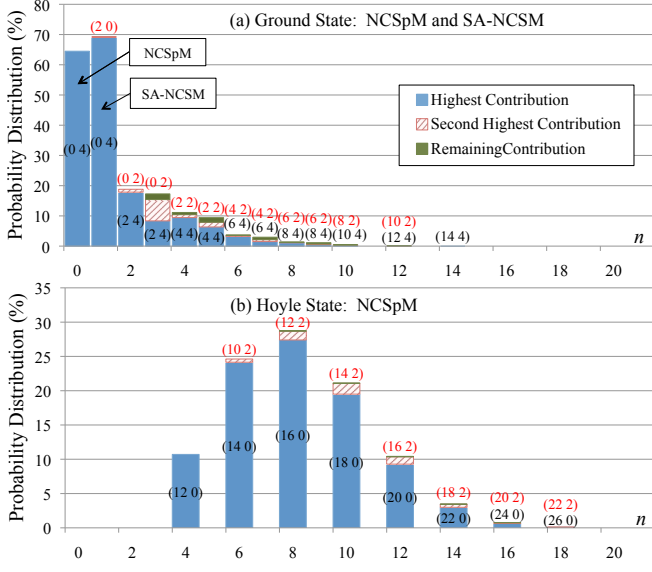


FIG. 3: Probability distribution for  $^{12}\text{C}$  as a function of the  $n$  total excitations, (a) of the lowest  $0^+$  state as calculated by the NCSpM (left) and the SA-NCSM (right), and (b) of the Hoyle state as calculated by the NCSpM. The dominant shape deformations, specified by  $(\lambda\mu)$ , are also shown.

formation of this state (see also  $Q$  of its  $2^+$  excitation in the next section) supports an underlying alpha-particle cluster structure of this  $0^+$  state and its rotational band.

It is interesting to point out that the  $4\hbar\Omega$  4p-4h (120) places the controversial  $2^+$  excitation within the lower region of the 9.6-12 MeV range of observations [2–6]. For comparison, recent *ab initio*  $N_{\text{max}} = 8$  NCSM calculations, while achieving a remarkable reproduction of the *g.st.* rotational band, yield the second  $0^+$  and  $2^+$  states around 13 MeV and 15 MeV, respectively [10], thus believed not to be associated with the Hoyle state but with higher-lying states of that spin-parity. Indeed, consistent with current *ab initio* observations, the NCSpM outcome demonstrates a large sensitivity of the energy of the Hoyle state and its  $2^+$  excitation on the model space (Fig. 4a).

Furthermore, a study of the effect of  $\gamma$  on the  $^{12}\text{C}$  energy spectrum (Fig. 4b) reveals that the additional degree of freedom associated with the  $\gamma$  model parameter is in fact substantially limited by the lowest  $0^+$  states (with only a small effect on the *g.st.* rotational band). Indeed, given the dramatic variation with  $\gamma$  for the  $0_2^+$  and  $0_3^+$  (Fig. 4b, insert), there is only a small window of reasonable  $\gamma$  values where observables are also found in agreement with experiment, as shown in the next section.

Finally, to show the important role of the  $2\hbar\Omega$  and  $4\hbar\Omega$  irreps considered in this study, we include additional  $S = 0$  symplectic irreps into the model space. In doing this, we indeed find no additional low-lying states for the  $\gamma$  parameter chosen here. For example, for  $2\hbar\Omega$  (24),  $4\hbar\Omega$  (82), (44), and (06),  $6\hbar\Omega$  (140), as well as  $8\hbar\Omega$  (160), the lowest state ( $0^+$ ) lies much higher than 18 MeV.

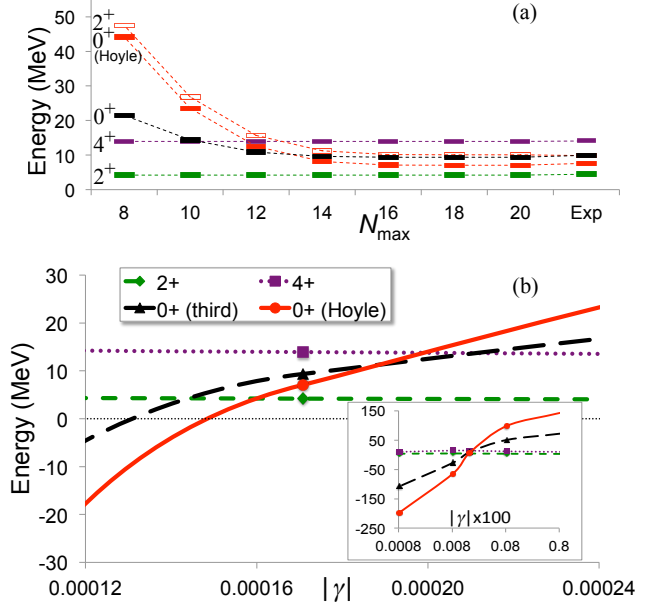


FIG. 4: Dependence of the  $^{12}\text{C}$  NCSpM energy spectrum on (a) the model space ( $N_{\text{max}}$ ) for  $\gamma = -1.71 \times 10^{-4}$  and (b) the  $\gamma$  model parameter for  $N_{\text{max}} = 20$ .

**Additional observables.** – The model with the selected  $\gamma = -1.71 \times 10^{-4}$  successfully reproduces other observables for  $^{12}\text{C}$  that are informative of the state structure, such as  $r_{\text{rms}}$  point-particle matter rms radii,  $Q$  electric quadrupole moments (Table I) and  $B(E2)$  transition strengths (Fig. 2a) [in general, for  $\gamma$  from  $-0.01$  to  $-10^{-5}$ , e.g.,  $r_{\text{rms}}$  for  $0_{g.st.}^+$  and  $0_2^+$  increases 1.4 times, as well as  $B(E2; 2_1^+ \rightarrow 0_{g.st.}^+)$  and  $Q_{2_1^+}$  increase four times]. However, nonzero  $B(E2; 0_2^+ \rightarrow 2_1^+)$  and  $M(E0; 0_2^+ \rightarrow 0_1^+)$  strengths can only result from mixing of  $\text{Sp}(3, \mathbb{R})$  irreps, which requires an  $\text{Sp}(3, \mathbb{R})$  symmetry-breaking interaction. But this can enter perturbatively. Indeed, a useful information on these quantities can be derived from a toy model that mixes the (120) irrep into the (04) irrep of the *g.st.* and that reveals that less than a 2% mixing can already yield the correct order of magnitude, namely,  $B(E2; 0_2^+ \rightarrow 2_1^+) = 8.7$  W.u. and  $M(E0; 0_2^+ \rightarrow 0_1^+) = 2.04$   $e\text{fm}^2$  as compared to experiment, 8.0(11) W.u. and 5.4(2)  $e\text{fm}^2$ , respectively.

We also find matter rms radius for the ground state (Table I) close to the value deduced from experiment in Ref. [31]. Interestingly, our calculations yield matter  $r_{\text{rms}} = 2.93$  fm for the Hoyle state. While this result drastically differs from predictions of cluster models [7, 34, 35], it is close to a recent value deduced from the experiment, 2.89(4) fm [33]. The NCSpM outcome yields a  $2_1^+$  electric quadrupole moment very close to the experimental value, and a large negative one for the  $2^+$  above the Hoyle state (Table I) indicating a substantial prolate deformation for the Hoyle and  $2^+$  states. Such a

TABLE I: Point-particle rms matter radii (fm) and electric quadrupole moments ( $e \text{ fm}^2$ ) for  $^{12}\text{C}$  and  $^{24}\text{Mg}$ . Experimental data taken from: <sup>a</sup>Ref. [31], <sup>b</sup>Ref. [32], <sup>c</sup>Ref. [33], <sup>d</sup>Ref. [29].

	State	NCSpm	Expt.	NCSpm	Expt.
	$^{12}\text{C}$			$^{24}\text{Mg}$	
matter	$0_{gs}^+$	2.44	2.43(2) <sup>a</sup>	$0_{gs}^+$	3.03
$r_{\text{rms}}$ (fm)	$0_2^+$ (Hoyle)	2.93	2.89(4) <sup>c</sup>	$0_{(4p4h)}^+$	3.26
	$0_3^+$	2.78		$0_{(2p2h)}^+$	3.17
$Q_{2+}$	$2_1^+$	+6.63	+6(3) <sup>d</sup>	$2_1^+$	-22.7
( $e \text{ fm}^2$ )	$2^+$ of $0_2^+$	-20.6		$2_{(4p4h)}^+$	-38.9

prolate deformation, albeit not so pronounced, has been also suggested by the *ab initio* lattice EFT [11].

**NCSpm applications to other nuclei.** — The outcome of the present analysis is not limited to  $^{12}\text{C}$ . The model we find is also applicable to low-lying states of other light nuclei, and, in particular, we show here the *g.st.* rotational band and low-lying  $0^+$  states of  $^{24}\text{Mg}$  (Fig. 2b). These states together with associated observables (see also Table I) are well described by the NCSpm with  $\gamma = -0.67 \times 10^{-4}$  in an  $N_{\text{max}} = 24$  model space using only a few spin-zero symplectic irreps, namely,  $0\hbar\Omega$   $0p$ - $0h$  (84) for the *g.st.* rotational band,  $0\hbar\Omega$  (46), (62), and (08),  $2\hbar\Omega$   $2p$ - $2h$  (142), as well as  $4\hbar\Omega$   $4p$ - $4h$  (200). This points to the efficacy and extensibility of the fully microscopic NCSpm model, which has indeed captured most of the important physics.

In short, we carried forward a no-core shell-model study with a schematic many-nucleon interaction to further unveil the underlying physics behind various phenomena important to the low-energy nuclear dynamics of  $^{12}\text{C}$ . We showed, for the first time, how both collective states and states suggested to have cluster-like substructures emerge out of a fully microscopic, shell-model framework, thereby providing a novel and essential perspective on the controversial Hoyle state.

This work was supported by the U.S. NSF (OCI-0904874), the U.S. DOE (de-sc0005248 & FG02-95ER-40934), and the SURF ACD acknowledges support by the U.S. NSF (grant 1004822) through the REU Site in Dept. of Physics & Astronomy at LSU. We acknowledge NERSC and LONI for providing HPC resources.

[1] H. O. U. Fynbo *et al.*, Nature 433, 136 (2005).  
[2] M. Freer *et al.*, Phys. Rev. C 76, 034320 (2007); M. Freer *et al.* *ibid.* 80, 041303 (2009).  
[3] S. Hyldegaard *et al.*, Phys. Rev. C 81, 024303 (2010).  
[4] M. Itoh *et al.*, Phys. Rev. C 84, 054308 (2011).  
[5] W. R. Zimmerman, N. E. Destefano, M. Freer, M. Gai, and F. D. Smit, Phys. Rev. C 84, 027304 (2011).

[6] Ad. R. Raduta *et al.*, Phys. Letts. B 705, 65 (2011).  
[7] M. Chernykh, H. Feldmeier, T. Neff, P. von Neumann-Cosel, and A. Richter, Phys. Rev. Lett. 98, 032501 (2007).  
[8] D. T. Khoa, D. C. Cuonga, Y. Kanada-En'yo, Phys. Letts. B 695, 469 (2011).  
[9] A. S. Umar, J. A. Maruhn, N. Itagaki, and V. E. Oberacker, Phys. Rev. Lett. 104, 212503 (2010).  
[10] R. Roth, J. Langhammer, A. Calci, S. Binder, and P. Navrátil, Phys. Rev. Lett. 107, 072501 (2011).  
[11] E. Epelbaum, H. Krebs, D. Lee, and Ulf-G. Meissner, Phys. Rev. Lett. 106, 192501 (2011); E. Epelbaum *et al.*, 1208.1328 (2012).  
[12] P. J. Ellis and T. Engeland, Nucl. Phys. A144, 161 (1970); T. Engeland and P. J. Ellis, Nucl. Phys. A181, 368 (1972).  
[13] T. Dytrych, "The Symmetry-Adapted NCSM Code," Louisiana State University, 2011 (unpublished).  
[14] A. M. Shirokov, J. P. Vary, A. I. Mazur, and T. A. Weber, Phys. Letts. B 644, 33 (2007).  
[15] G. Rosensteel and D. J. Rowe, Phys. Rev. Lett. 38, 10 (1977).  
[16] T. Dytrych, K. D. Sviratcheva, C. Bahri, J. P. Draayer, and J. P. Vary, Phys. Rev. Lett. 98, 162503 (2007).  
[17] C. Bahri and D. J. Rowe, Nucl. Phys. A 662, 125 (2000).  
[18] A. Bohr and B. R. Mottelson, *Mat. Fys. Medd. Dan. Vid. Selsk.* 27, No. 16 (1953); B. R. Mottelson, Nobel Lectures, Physics 1971-1980, World Scientific Publishing Co., Singapore (1992).  
[19] J. P. Elliott, Proc. Roy. Soc. A245, 128 (1958); *ibid.* A245, 562 (1958); J. P. Elliott and M. Harvey, *ibid.* A272, 557 (1962).  
[20] T. Dytrych, K. D. Sviratcheva, J. P. Draayer, C. Bahri, and J. P. Vary, J. Phys. G: Nucl. Part. Phys. 35, 123101 (2008).  
[21] P. Navrátil, J. P. Vary, and B. R. Barrett, Phys. Rev. Lett. 84, 5728 (2000).  
[22] M. Harvey, Adv. Nucl. Phys. 1, 62 (1968).  
[23] O. Castaños and J. P. Draayer, Nucl. Phys. A491, 349 (1989).  
[24] G. Rosensteel and J. P. Draayer, Nucl. Phys. A436, 445 (1985).  
[25] D. J. Rowe, Phys. Rev. 162, 866 (1967).  
[26] D. J. Rowe, G. Thiamova, and J. L. Wood, Phys. Rev. Lett. 97, 202501 (2006).  
[27] D.R. Peterson and K.T. Hecht, Nucl. Phys. A344, 361 (1980).  
[28] R. Le Blanc, J. Carvalho, M. Vassanji, and D.J. Rowe, Nucl. Phys. A452, 263 (1986).  
[29] F. Ajzenberg-Selove and J.H. Kelley, Nucl. Phys. A506, 1 (1990); R.B. Firestone, Nuclear Data Sheets 108, 2319 (2007).  
[30] Y. Kanada-En'yo, Phys. Rev. Lett. 81, 5291 (1998).  
[31] I. Tanihata *et al.*, Phys. Rev. Lett. 55, 2676 (1985).  
[32] J. Veronotte, G. Berrier-Ronsin, J. Kalifa, and R. Tamisier, Nucl. Phys. A390, 285 (1982).  
[33] A. N. Danilov, T. L. Belyaeva, A. S. Demyanova, S. A. Goncharov, and A. A. Ogloblin, Phys. Rev. C 80, 054603 (2009).  
[34] Y. Funaki, A. Tohsaki, H. Horiuchi, P. Schuck, and G. Ropke, Phys. Rev. C 67, 051306 (2003).  
[35] T. Yamada and P. Schuck, Phys. Rev. C 69, 024309 (2004).